

Peaks theory and the excursion set approach

Aseem Paranjape^{1*} & Ravi K. Sheth^{1,2}

¹ *The Abdus Salam International Center for Theoretical Physics, Strada Costiera, 11, Trieste 34151, Italy*

² *Center for Particle Cosmology, University of Pennsylvania, 209 S. 33rd St., Philadelphia, PA 19104, USA*

13 August 2012

ABSTRACT

We describe a model of dark matter halo abundances and clustering which combines the two most widely used approaches to this problem: that based on peaks and the other based on excursion sets. Our approach can be thought of as addressing the cloud-in-cloud problem for peaks and/or modifying the excursion set approach so that it averages over a special subset, rather than all possible walks. In this respect, it seeks to account for correlations between steps in the walk as well as correlations between walks. We first show how the excursion set and peaks models can be written in the same formalism, and then use this correspondence to write our combined excursion set peaks model. We then give simple expressions for the mass function and bias, showing that even the linear halo bias factor is predicted to be k -dependent as a consequence of the nonlocality associated with the peak constraint. At large masses, our model has little or no need to rescale the variable δ_c from the value associated with spherical collapse, and suggests a simple explanation for why the linear halo bias factor appears to lie above that based on the peak-background split at high masses when such a rescaling is assumed. Although we have concentrated on peaks, our analysis is more generally applicable to other traditionally single-scale analyses of large-scale structure.

Key words: large-scale structure of Universe

1 INTRODUCTION

Press & Schechter (1974) argued that the abundance of nonlinear virialized objects at late times (such as the present) should be sensitive to the statistics of the initial fluctuation field, and to the subsequent expansion history of the universe. This is the basis for studies which seek to use the abundance and clustering of galaxy clusters to constrain cosmological parameters.

Their work has motivated the study of analytical models for the formation, and hence the abundance and spatial distribution, of halos, which can be used to provide fitting formulae when interpreting data. Following Sheth & Tormen (1999), the most widely used fitting formulae are self-similar, in the sense that the predicted halo abundances can be scaled to a universal form which is independent of cosmology, redshift and power spectrum. This vastly simplifies cosmological analyses. (This universality is only expected to hold approximately, and the

next generation of datasets may have sufficiently many clusters that departures from universality must be accounted for. We will have more to say about this later.)

The self-similar functional form can be derived from a physically motivated model of collapse (Sheth, Mo & Tormen, 2001). The number density dn/dm of halos in the mass range $(m, m+dm)$ is written as

$$\frac{m}{\bar{\rho}} \frac{dn(m)}{dm} dm = f(\nu) d\nu, \quad (1)$$

where $\bar{\rho}$ is the background density and $\nu = \delta_c/\sigma$, with δ_c the rescaled time variable and σ the rescaled mass variable ($\sigma^2(m) \equiv \langle \delta^2(m) \rangle$ is the variance of the matter density field smoothed on a Lagrangian length scale corresponding to mass m and linearly extrapolated to present day). Universality is manifest in the statement that f depends only on ν , but, unfortunately, the most naive use of this form predicts too few massive clusters. This has motivated the following ad-hoc approach: one actually fits $f(\sqrt{q}\nu)$ to the data, and determines q from

* E-mail: aparanja@ictp.it

the fit. This semi-empirical approach has worked rather well, in the sense that q appears to be approximately independent of cosmology, redshift and power spectrum, although recent simulations are beginning to show departures from universality (Bagla et al., 2009).

Since observations will soon deliver large cluster catalogs over a range of redshifts, it is clearly desirable to have a more fundamental understanding of why $q \neq 1$, particularly because, on an object by object basis, the physical model of collapse almost never has $\delta < \delta_c$. I.e., $q < 1$ appears to arise in the step which converts from the physics of halo formation to a statistical description of halo abundances (Sheth et al., 2001). One of the main goals of this paper is to provide some insight into the origin of this factor.

To do so, we revisit the two most common models for identifying halos from the initial fluctuation field: the peaks theory of Bardeen et al. (1986, hereafter BBKS), and the excursion set approach of Bond et al. (1991). Although both make predictions which can be phrased in terms of the self-similar variable ν , and both treat ν as the ratio of δ_c/σ , the former treats the numerator of this ratio as the stochastic quantity, whereas for the latter, it is the denominator which can vary. They also differ fundamentally in their approach to the problem. Peaks theory seeks to describe the point process which describes the special positions in the initial conditions around which halos collapse. The excursion set approach aims only at a statistical description of the mass fraction in bound objects, and assumes that this can be done by consideration of all points in space – not just the special ones around which halos form. Our analysis below shows how to merge the two descriptions.

Section 2 shows that the excursion set and peaks models can be written in the same formalism, and then describes our excursion set model for peaks, arguing that the result goes a substantial way towards explaining the origin of the factor of a . Section 3 extends this to describe the conditional function of excursion set peaks in constrained larger-scale environments, and from there builds a model for the large scale bias factors. This uses the recent work of (Musso, Paranjape & Sheth, 2012, hereafter MPS) to show that halo bias in our approach is generically expected to be k dependent. It also shows that at high masses, our new expression for halo bias is qualitatively similar to that seen in simulations, again suggesting that our excursion set peaks model of the origin of $a \neq 1$ is reasonable. A final section summarizes our results, discusses them in the context of previous work on the relationship between excursion sets and peaks, and suggests ways in which our approach could be improved further.

2 THE UNCONDITIONAL MASS FUNCTION

This section develops what we call the excursion set model for peaks: it is both a peaks model which deals with

different smoothing scales, and an excursion set model which deals with the statistics of special rather than random positions. This is particularly interesting because Sheth et al. (2001) have argued that the latter is a necessary change to the standard excursion set approach, and Ludlow & Porciani (2011) have argued that the correspondence between peaks in the initial conditions and halos at late times in their simulations is quite good.

2.1 Notation

Let $s(R)$ denote the variance of the (linearly extrapolated) density contrast δ smoothed on a Lagrangian length scale R . Then $s \equiv \sigma_0^2$ where

$$\sigma_j^2 = \int \frac{d^3k}{(2\pi)^3} P(k) k^{2j} W^2(kR) \quad (2)$$

and our notation has dropped the explicit dependence of σ_j on R , where we think no confusion will arise. Here $P(k)$ is the power spectrum of the field, and $W(kR)$ is the Fourier transform of the smoothing filter. For what follows, it is also convenient to define

$$R_* \equiv \sqrt{3}\sigma_1/\sigma_2 \quad \text{and} \quad \gamma \equiv \sigma_1^2/\sigma_0\sigma_2. \quad (3)$$

Unless stated otherwise, we will always consider Gaussian smoothing filters, for which $W(kR) = \exp(-k^2 R^2/2)$, and, for the $P(k)$ of current interest in cosmology, all the integrals above converge.

We return to the issue of smoothing filter in the Discussion section, because the analysis which follows exploits the following property which is special to Gaussian smoothing. Namely, the Laplacian of the field on a given smoothing scale $\nabla_{\mathbf{x}}^2 \delta(R, \mathbf{x})$, which is a quantity of fundamental importance in peaks theory, is the same as the derivative of the field with respect to smoothing scale, a fundamental quantity in excursion set theory.

On dimensional grounds, the volume associated with a smoothing filter is $V \propto R^3$; for a Gaussian filter $V = (2\pi R^2)^{3/2}$. It is natural to associate a mass with the smoothing scale R : $m \equiv \bar{\rho}V$, where $\bar{\rho}$ is the comoving background density. We will only consider hierarchical models in which the fluctuations in the initial field were small. The former means that σ_0 is a monotonically decreasing function of R , and the latter that R , m and σ_0 are equivalent variables. In what follows we illustrate our results using $P(k)$ for a flat Λ CDM cosmological model with parameters $(\Omega_m, \Omega_\Lambda, h, \sigma_8, n_s) = (0.25, 0.75, 0.7, 0.8, 0.95)$.

2.2 The excursion set approach

The excursion set approach assumes that the mass fraction associated with bound halos of mass m at any given time t equals the volume fraction of positions in the initial fluctuation field which, when smoothed on scale $R \propto m^{1/3}$, have overdensity $\delta(R) = \delta_c(t)$ and, for all $R' > R$, have $\delta(R') < \delta_c(t)$. This latter constraint is difficult to handle because it implies an infinite number of constraints (one for each smoothing scale).

Musso & Sheth (2012, hereafter MS) showed that the much simpler requirements that $\delta(R) > \delta_c$ and $\delta(R + \Delta R) < \delta_c$ for $\Delta R \ll 1$ (i.e., just one additional constraint) permit a simple analytic estimate of this fraction which is remarkably accurate. Although this fraction depends on the power spectrum of the underlying fluctuation field, much of this dependence can be removed if one works instead with the requirement $\delta(s) > \delta_c$ and $\delta(s - \Delta s) < \delta_c$ (recall that s and R are equivalent variables). Thus, if $v \equiv d\delta/ds$, then MS argued that the fraction $f(s)$ of interest satisfies

$$\Delta s f(s) \equiv \int_0^\infty dv \int_{\delta_c}^{\delta_c + v\Delta s} d\delta p(v, \delta), \quad (4)$$

where $p(v, \delta)$ is the joint distribution of δ and its derivative $v \equiv d\delta/ds$. Taking the limit $\Delta s \rightarrow ds \ll 1$ implies

$$f(s) \equiv \int_0^\infty dv v p(v, \delta_c), \quad (5)$$

We will see shortly that the issue is what exactly to use for $p(v, \delta)$.

The rms values of δ and v are σ_0 and $(2\gamma\sigma_0)^{-1}$, respectively. So, if we define

$$\nu \equiv \delta_c/\sigma_0 \quad \text{and} \quad x \equiv 2\gamma\sigma_0 v, \quad (6)$$

(our choice of notation will become clear shortly) and if we choose to average over all positions in the initial Gaussian random field which have height δ_c on scale s , then equation (5) implies that

$$sf(s) \equiv \frac{\exp(-\nu^2/2)}{2\gamma\sqrt{2\pi}} \int_0^\infty dx x p_G(x - \gamma\nu; 1 - \gamma^2) \quad (7)$$

where $p_G(y - \mu; s)$ a Gaussian distribution for variable y , with mean μ and variance s . The right hand side is clearly a function of the scaling variable ν and γ . The dependence on γ means that the result is not a completely universal function of ν , but MS argued that, over the range of power spectra of current interest in cosmology, this dependence is relatively weak. Therefore, it is useful to use the fact that $\nu f(\nu) = sf(s) |d \ln s / d \ln \nu| = 2sf(s)$ to write the expression above in terms of the scaling variable ν :

$$\nu f_{\text{MS}}(\nu) \equiv \frac{\nu \exp(-\nu^2/2)}{\sqrt{2\pi}} \frac{\langle x|\gamma, \gamma\nu \rangle_{\text{MS}}}{\gamma\nu}, \quad (8)$$

where

$$\langle x|\gamma, x_* \rangle_{\text{MS}} \equiv \int_0^\infty dx x p_G(x - x_*; 1 - \gamma^2). \quad (9)$$

This shows that $f(\nu)$ is the product of the Gaussian probability of having height ν and the mean ‘curvature’ associated with such positions. (This integral can be done analytically; see MS. Also, although we will not focus on the expected departures from universality in this model, which come from the dependence on γ , we would like to emphasize that small departures are predicted.)

MS showed that this expression, based on their ‘one-step’ approximation, provided an excellent description of the exact solution in which the constraint on the walk height is satisfied on all scales. While this is significant

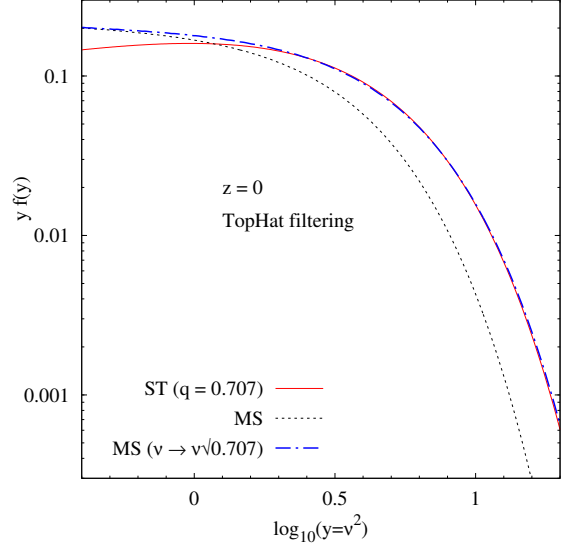


Figure 1. Mass function of halos identified in a Λ CDM simulation (solid red; Sheth & Tormen, 1999, with their $q = 0.707$) and as predicted by the excursion set approach (Musso & Sheth, 2012) (dotted black) and with $\nu \rightarrow \sqrt{0.707}\nu$ (dot-dashed blue) in equation (8). This plot uses TopHat filtering of the Λ CDM power spectrum.

– it effectively solves the same excursion set problem for ‘correlated’ steps that Bond et al. (1991) solved for ‘uncorrelated’ steps – it does not really solve the problem as stated at the beginning of this sub-section. Namely, the quantity of interest is a volume fraction in the initial field. One should estimate this by averaging over the full set of walks in one realization of the field. But what has actually been calculated is an ergodic average over an ensemble of walks in which the steps in each walk are correlated, but the walks themselves are independent of one another. Sheth et al. (2001) demonstrated that this replacement is incorrect; in fact, one must either account for the correlations between walks, or account for the fact that the set of walks over which one should average is a special subset of all walks (also see Sheth, 2011; Paranjape, Lam & Sheth, 2012).

Figure 1 provides one illustration of why the distinction matters. (For this plot only, we have used a Tophat, rather than Gaussian, filter in all integrals over $P(k)$.) The solid curve shows the fitting function of Sheth & Tormen (1999)

$$\nu f_{\text{ST}}(\nu) = 0.644 \left[1 + (q\nu^2)^{-0.3} \right] \frac{\sqrt{q\nu^2} \exp(-q\nu^2/2)}{\sqrt{2\pi}} \quad (10)$$

which provides a good description of halo counts in simulations. As mentioned in the Introduction, this function is expressed in terms of the scaling variable $\sqrt{q}\nu$, where ν is the same quantity which enters in the excursion set approach and $q \approx 0.7$. The dotted curve shows equation (8); it vastly underestimates the halo counts at large ν .

It is easy to see why this happens. At $\nu^2 \gg 1$, $\nu f_{\text{ST}}(\nu) \rightarrow 0.644\sqrt{q\nu^2} \exp(-q\nu^2/2)\sqrt{2\pi}$ whereas equation (8) becomes $\nu f_{\text{MS}}(\nu) \rightarrow \nu \exp(-\nu^2/2)/\sqrt{2\pi}$. This shows that if we rescale $\nu \rightarrow \sqrt{q}\nu$ in equation (8), then the result should provide a good description of the halo counts, upto the difference in amplitude of 0.644. However, even this difference in amplitude can be accounted for by noting that the term in square brackets in equation (10) only equals unity at very large ν . At $\nu^2 = 10$, it is $\approx 3/2$, so multiplying by 0.644 yields unity. The dot-dashed curve shows that, indeed, rescaling $\nu \rightarrow \sqrt{0.707}\nu$ in equation (8) works very well.

Note that $q < 1$ is required to achieve this agreement at large ν . While it is tempting to associate this rescaling with a reduction in the value of δ_c , this is problematic because direct measurements of the overdensity in patches which are destined to form halos show that the critical density required for collapse increases at small ν . This increase is qualitatively consistent with expectations based on modelling halo formation using a triaxial rather than spherical collapse (Sheth et al., 2001). I.e., the physics of halo formation suggests that, if we want to think of the parameter q as rescaling δ_c , then q should be greater, rather than less than unity. The alternative, which we will not explore further here (but see discussion in Paranjape et al., 2012), is to assume that \sqrt{q} rescales σ rather than δ_c . Rather, the next section explores a quite different reason for why rescaling with $q < 1$ works so well. The main point we wish to make here is that, absent an understanding of why rescaling ν was necessary, one should not use the shape of $f(\nu)$ to make conclusions about whether the physics of collapse was spherical or not; the evidence for triaxial collapse comes from the direct measurements of the properties of the patches from which halos formed (i.e., those in Sheth et al., 2001).

2.3 Peaks in the initial field

In the argument which led to equation (8), we noted that the predicted mass fraction $f(\nu)$ depends critically on what one chooses for $p(\nu|\delta_c)$. In what follows, we will show what happens if we wish to add the additional constraint that, on scale s , $\delta = \delta_c$ is also a local maximum of the field.

The number density of peaks of height δ depends critically on the smoothing scale on which the peaks were defined. If σ_0 denotes the rms value of the density fluctuation on the chosen smoothing scale, then the number density of peaks of scaled height $\nu = \delta/\sigma_0$ in a Gaussian-smoothed Gaussian random field is

$$\mathcal{N}_{\text{pk}}(\nu) = \int dx \mathcal{N}_{\text{pk}}(x, \nu) = \frac{e^{-\nu^2/2}}{\sqrt{2\pi}} \frac{G_0(\gamma, \gamma\nu)}{(2\pi R_*^2)^{3/2}}, \quad (11)$$

where γ and R_* were defined earlier, and

$$G_J(\gamma, x_*) \equiv \int_0^\infty dx x^J F(x) p_G(x - x_*; 1 - \gamma^2), \quad (12)$$

with

$$F(x) = \frac{1}{2} (x^3 - 3x) \left\{ \text{erf} \left(x\sqrt{\frac{5}{2}} \right) + \text{erf} \left(x\sqrt{\frac{5}{8}} \right) \right\} + \sqrt{\frac{2}{5\pi}} \left[\left(\frac{31x^2}{4} + \frac{8}{5} \right) e^{-5x^2/8} + \left(\frac{x^2}{2} - \frac{8}{5} \right) e^{-5x^2/2} \right], \quad (13)$$

(equations A14–A19 in BBKS). The variable x is the Laplacian of the field normalized by its rms value (for Gaussian filters, this rms is σ_2), so it represents the curvature around the peak position. Therefore, $F(x)$ quantifies how different the set of curvatures is around a peak position compared to a randomly placed one.

To map from peak number densities to halo mass fractions, one must associate a mass with each peak. The natural choice is the mass m contained within the smoothing window: $m = \bar{\rho}V$ with $V \propto R^3$. But this has the unfortunate consequence that peaks of different height ν will all have the same mass, whereas the intuitive expectation is that more massive objects should be associated with higher peaks.

I.e., the intuitive picture is one in which there is a critical density contrast δ_c which is associated with halos (in what follows we will set $\delta_c = 1.686$, thus ignoring the mild dependence on cosmology predicted by the spherical collapse model), and massive halos have large $\nu = \delta_c/\sigma_0$ because they have small σ_0 (this is what happens naturally in the excursion set approach). Thus, the main difficulty in identifying peaks with halos is that equation (11) is defined for a fixed smoothing scale R (so changes in ν are due to changes in δ), whereas one would really like to allow R to vary instead.

If one assumes naively (and incorrectly) that ν in equation (11) has δ_c fixed and R varying, then one might naively (and incorrectly) assume that the mass fraction of the Universe that is in peaks of mass m is given by

$$f_{\text{BBKS}}(\nu) = \frac{m}{\bar{\rho}} \mathcal{N}_{\text{pk}}(\nu) = \frac{e^{-\nu^2/2}}{\sqrt{2\pi}} \frac{V}{V_*} G_0(\gamma, \gamma\nu), \quad (14)$$

where we have defined $V_* = (2\pi R_*^2)^{3/2}$. Quite apart from the mathematical inconsistency associated with making this assumption, there is a conceptual difficulty which is known as the cloud-in-cloud problem. This comes from considering how the density around a given position fluctuates as one changes the smoothing scale R . One might imagine that a given position is a peak on some smoothing scales and not on others; or that a position which is a local maximum of height ν on a small smoothing scale may have an even larger value of ν on a large smoothing scale, without being a local maximum of the field on the larger smoothing scale. Which, if any of these cases, should one associate with halos?

2.4 Excursion set peaks

As MS noted, the excursion set approach of the previous section shows how one might address this problem more

consistently. Namely, it says that of the peaks present on scale s , we want those which have a smaller height on the next larger smoothing scale. Therefore, the same logic which led to equation (7) (i.e., demanding that the scaled peak height lie between $\nu = \delta_c/\sigma_0$ and $\nu + (x/2\gamma)\Delta \ln s$) will now yield

$$\mathcal{N}_{\text{ESP}}(\nu) = \frac{1}{\gamma\nu} \int_0^\infty dx x \mathcal{N}_{\text{pk}}(\nu, x), \quad (15)$$

making

$$f_{\text{ESP}}(\nu) = \frac{e^{-\nu^2/2}}{\sqrt{2\pi}} \frac{V}{V_*} G_0(\gamma, \gamma\nu) \frac{\langle x|\gamma, \gamma\nu \rangle_{\text{ESP}}}{\gamma\nu}, \quad (16)$$

where

$$\langle x|\gamma, x_* \rangle_{\text{ESP}} = G_1(\gamma, x_*)/G_0(\gamma, x_*). \quad (17)$$

(This is where the choice of a Gaussian for the smoothing filter simplifies the analysis, since a constraint on the value of the derivative with respect to smoothing scale becomes a constraint on the curvature of the field. This also explains why, in equation (6) we used x to denote $d\delta/ds$ normalized by its rms value.)

Essentially this same formula for peaks, equation (16), has appeared previously (Appel & Jones, 1990). However, we believe our treatment highlights the similarities and differences between peaks and random positions more clearly. In particular, notice that f_{ESP} modifies the peaks probability in the same way that f_{MS} modifies the gaussian pdf: the distribution of peaks picks up an additional factor of the normalised mean *peak* curvature. In this respect, the only conceptual difference between f_{ESP} and f_{MS} is that the latter averages over ‘random’ positions in the field, whereas the former averages over ‘special’ ones. In other words, f_{ESP} addresses both the cloud-in-cloud problem for peaks (the fundamental failing of the peaks approach), and the question of how the excursion set predictions are modified if one averaged over special positions in the initial field (the fundamental failing of the excursion set approach).

The analysis above shows that changing the ensemble over which the excursion set average is computed has a dramatic effect. To see this explicitly note that, at large $\nu \gg 1$, $G_0 \rightarrow \gamma^3(\nu^3 - 3\nu)$ and $\langle x|\gamma, \gamma\nu \rangle_{\text{ESP}} \rightarrow \gamma\nu$. This makes

$$f_{\text{ESP}}(\nu) \rightarrow \frac{e^{-\nu^2/2}}{\sqrt{2\pi}} (\nu^3 - 3\nu) \frac{V\gamma^3}{V_*} \approx f_{\text{MS}}(\nu) \frac{V\gamma^3\nu^3}{V_*}. \quad (18)$$

For $P(k) \propto k^n$, $\gamma^3 V/V_* = [(n+3)/6]^{3/2}$ is just a constant independent of m , so $f_{\text{ESP}}/f_{\text{MS}} \rightarrow [\nu^2(n+3)/6]^{3/2}$; this grows rapidly at large ν . We will return to this shortly.

Figure 2 compares these different models for halos using Gaussian filtering of the same Λ CDM spectrum as before. The curves show the results for BBKS (dashed blue), MS (dotted black) and ESP (solid red). The dashed blue curve is anecdotal, since, as we argued, it is not well motivated. We have included it to illustrate that the difference between it and the more careful calculation (ESP) is small at large masses.

The real interest in this plot is the fact that, at large

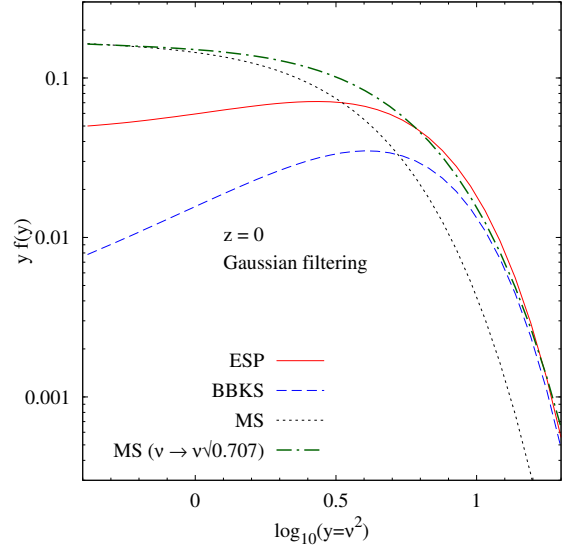


Figure 2. Mass functions with Gaussian filtering of a Λ CDM spectrum in the three formalisms discussed in the text: peaks (equation 14, dashed blue), excursion sets (equation 8, dotted black) and ESP (equation 16, solid red). The dot-dashed green curve shows equation (8) with $\nu \rightarrow \sqrt{0.707}\nu$; at large ν , it is quite similar to ESP. As discussed in the text, the dashed blue curve for peaks is not well motivated and is only shown for comparison with the more appropriate ESP curve.

masses, f_{MS} lies about an order of magnitude below f_{ESP} . Although we argued that this is expected (equation 18), it is interesting to consider this in view of our remarks in the Introduction about the discrepancy between the usual excursion set prediction and halo abundances in simulations. We noted that to fit halo abundances it was common to scale the usual excursion set prediction (i.e. f_{MS}) by setting $\nu \rightarrow a\nu$, with $a \sim \sqrt{0.707}$ (e.g. our Figure 1). The dot-dashed green curve in Figure 2 shows that setting $\nu \rightarrow \sqrt{0.707}\nu$ in equation (8) brings it into remarkably better agreement with f_{ESP} ; values of a between $0.7 \sim 0.8$ also do well. This strongly suggests that much of the discrepancy between the usual excursion set predictions and halo abundances in simulations can be attributed to inappropriate averaging in the excursion set approach. We show in the next section that this has interesting consequences for the predicted spatial distribution of halos.

2.5 Excursion set peaks with moving barriers

Before moving on to the study of predicted halo bias, it is worth noting that this approach makes it particularly easy to see how to incorporate the effects of a scale dependent δ_c . E.g., if we set $\delta_c \rightarrow B(s)$, then

$$\mathcal{N}_{\text{ESP}}(\nu) = \frac{1}{\gamma\nu} \int_{2\gamma\sigma_0 B'}^\infty dx (x - 2\gamma\sigma_0 B') \mathcal{N}_{\text{pk}}(B/\sigma_0, x). \quad (19)$$

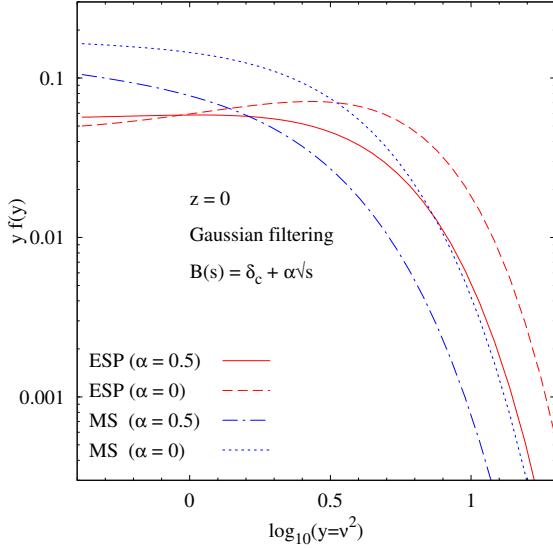


Figure 3. Mass functions with Gaussian filtering of a Λ CDM spectrum for barrier shapes of the type $B(s) = \delta_c + \alpha\sqrt{s}$, for excursion sets and ESP. The curves show ESP (red) for $\alpha = 0.5$ (solid, following from equation 19) and $\alpha = 0$ (dashed, equation 16), and the MS result (blue) for $\alpha = 0.5$ (dot-dashed, their equation 5) and $\alpha = 0$ (dotted, equation 8).

In models of triaxial (rather than spherical) collapse, it is a good approximation to set $B(s) \approx \delta_c + \alpha\sqrt{s}$ (Sheth et al., 2001), making $B/\sigma_0 = \nu + \alpha$ and $2\gamma\sigma_0 B' = \gamma\alpha$. Figure 3 compares this model with $\alpha = 0.5$ (see Moreno et al. 2009 for why this value is interesting) with the case in which $\alpha = 0$ ($B = \delta_c$ is constant). This shows that while the shape of $f(\nu)$ is indeed sensitive to the physics of collapse, this sensitivity can only be used as a diagnostic if one is confident that the statistical prediction has been based on the correct ensemble average.

3 CONDITIONAL MASS FUNCTIONS AND HALO BIAS

MS noted that it was straightforward to extend their analysis to make models of the mass fraction in halos of mass m (corresponding to variance $s = \sigma_0^2(R)$ with $R \propto m^{1/3}$) which are constrained to lie within regions of some specified size R_0 (corresponding to variance $S_0 = \sigma_0^2(R_0)$) and overdensity δ_0 . An explicit expression for the conditional mass fraction, which is associated with the unconditional one in equation (8) has recently been provided by Musso et al. (2012, MPS).

It is instructive to rewrite their result in the notation of BBKS, who provided a similar analysis for peaks. Using the dictionary given in Appendix A1, equation (28) of MPS can be written as

$$d\nu f_{\text{MPS}}(\nu|\delta_0, S_0) = d\nu_p \frac{e^{-\nu_p^2/2}}{\sqrt{2\pi}} \frac{\langle x|\tilde{\gamma}, \tilde{\gamma}\tilde{\nu} \rangle_{\text{MS}}}{\gamma\nu}, \quad (20)$$

with $\langle x|\gamma, x_* \rangle_{\text{MS}}$ defined in equation (9), and the

BBKS quantities $\{\nu_p, \tilde{\gamma}, \tilde{\nu}\}$ given in equations (A1), (A2) and (A3).

Exactly the same logic as before, when applied to the BBKS expression for peaks conditioned on having δ_0 on scale S_0 (equation E11 of BBKS), leads to

$$d\nu f_{\text{ESP}}(\nu|\delta_0, S_0) = d\nu_p \frac{e^{-\nu_p^2/2}}{\sqrt{2\pi}} \frac{V}{V_*} G_0(\tilde{\gamma}, \tilde{\gamma}\tilde{\nu}) \times \frac{\langle x|\tilde{\gamma}, \tilde{\gamma}\tilde{\nu} \rangle_{\text{ESP}}}{\gamma\nu}, \quad (21)$$

with $\langle x|\gamma, x_* \rangle_{\text{ESP}}$ defined in equation (17).

3.1 Halo bias

MPS argued that a useful way of defining bias coefficients for a Gaussian field is to cross-correlate the density of the biased tracers with Hermite polynomials in the matter overdensity. The former is defined as the ratio of the conditional and unconditional mass fractions

$$\langle \rho_h|\delta_0 \rangle = f(\nu|\delta_0, S_0)/f(\nu), \quad (22)$$

and MPS showed that applying this prescription to the excursion sets result (equations 20 and 8) leads to closed-form expressions for the bias coefficients:

$$\begin{aligned} b_n &\equiv S_0^{-n/2} \left\langle \rho_h H_n(\delta_0/\sqrt{S_0}) \right\rangle \\ &= S_0^{-n/2} \int_{-\infty}^{\infty} d\delta_0 p_G(\delta_0; S_0) \langle \rho_h|\delta_0 \rangle H_n(\delta_0/\sqrt{S_0}), \end{aligned} \quad (23)$$

where $H_n(x) = e^{x^2/2}(-d/dx)^n e^{-x^2/2}$ are the “probabilist’s” Hermite polynomials.

MPS also showed that these b_n have the structure

$$b_n = \left(\frac{S_\times}{S_0} \right)^n \sum_{r=0}^n \binom{n}{r} b_{nr} \epsilon_\times^r, \quad (24)$$

where S_\times and ϵ_\times are given in equation (A5), and that the scale-independent (but mass-dependent) b_{nr} could be naturally interpreted as bias coefficients in *Fourier* space, with connections to the work of Szalay (1988) and Matsubara (2011). They also showed that, at least for $n = 1, 2$, the b_{nr} satisfy some remarkable linear relations between each other: for fixed n , all the b_{kr} with $1 \leq r \leq k \leq n$ can be written as linear combinations of b_{k0} , $1 \leq k \leq n$. More surprisingly, they showed that the peaks bias parameters at linear and quadratic order derived by Desjacques et al. (2010) *also* satisfied exactly the same linear relations between coefficients, although the form of the coefficients themselves was different.

Our results above allow us to generalise the connection between peaks and excursion sets bias to *all* orders. Notice that the quantity $\langle \rho_h|\delta_0 \rangle = f(\nu|\delta_0, S_0)/f(\nu)$ is given by

$$\langle \rho_h|\delta_0, S_0 \rangle = \frac{d\nu_p e^{-\nu_p^2/2}/\sqrt{2\pi}}{d\nu e^{-\nu^2/2}/\sqrt{2\pi}} \frac{G_J(\tilde{\gamma}, \tilde{\gamma}\tilde{\nu})}{G_J(\gamma, \gamma\nu)}. \quad (25)$$

This expression applies to all three formalisms with appropriate choices for $F(x)$ and J : for excursion sets

$F(x) = 1$, $J = 1$, while for peaks and ESP we use equation (13) for $F(x)$, with $J = 0$ for peaks and $J = 1$ for ESP. As a result, the only real difference between $\langle \rho_h | \delta_0 \rangle$ defined for peaks, excursion sets or the ESP extension is in the choice of the curvature function $F(x)$. This function is independent of δ_0 and simply goes for a ride in the series expansion that defines the bias coefficients. More precisely, the MPS result, that the b_n are Taylor coefficients of the expansion of $\langle \rho_h | \delta_0, \tilde{c} = 0 \rangle$ in powers of δ_0 (where \tilde{c} is the matrix given in equation A6), relied only on the properties of the Gaussian $\sim e^{-\nu^2/2} p_G(x - \tilde{\gamma}\nu; 1 - \tilde{\gamma}^2)$ and not on the fact that they were analysing the special case $F(x) = 1$. This result therefore applies equally well to peaks theory and its extension.

This allows us to generalise the results in Appendix A of MPS trivially. We show how to do this in Appendix A2, and we find

$$\delta_c b_n = \left(\frac{S_\times}{S_0} \right)^n \sum_{k=0}^n \binom{n}{k} (1 - \epsilon_\times)^k \lambda_k \mu_{n-k}, \quad (26)$$

with the ν -dependent quantities μ_k and λ_k defined as

$$\mu_k \equiv \nu^k H_k(\nu) ; \quad \lambda_k \equiv (-\Gamma\nu)^k \langle H_k(y - \Gamma\nu) \rangle_F, \quad (27)$$

where $\Gamma^2 \equiv \gamma^2/(1 - \gamma^2)$ and the F -averaged Hermite polynomial is

$$\begin{aligned} & \langle H_k(y - y_*) \rangle_F \\ & \equiv \frac{\int_0^\infty dy y^J F(y\gamma/\Gamma) p_G(y - \Gamma\nu; 1) H_k(y - y_*)}{\int_0^\infty dy y^J F(y\gamma/\Gamma) p_G(y - \Gamma\nu; 1)}. \end{aligned} \quad (28)$$

It is straightforward to check that setting $F(x) = 1$, $J = 1$ recovers the results of MPS, while setting $J = 0$ and using equation (13) with $n = 1, 2$ recovers those of Desjacques et al. (2010). More interestingly, equation (26) can be rearranged to write equation (24) with

$$\delta_c b_{nr} = (-1)^r \sum_{k=r}^n \binom{n-r}{k-r} \mu_{n-k} \lambda_k. \quad (29)$$

The μ_k are independent of the function $F(x)$, so that it is useful to set $r = 0$ and re-express the F -dependent λ_k in terms of the peak-background split parameters b_{n0} . Using $\mu_0 = 1 = \lambda_0$ we can write $\delta_c b_{n0} - \mu_n = \sum_{k=1}^n D_{nk} \lambda_k$, where $D_{nk} \equiv \binom{n}{k} \mu_{n-k}$ is an invertible lower-triangular matrix with diagonal elements unity, and we find

$$\begin{aligned} \lambda_1 &= \delta_c b_{10} - \mu_1, \\ \lambda_n &= \delta_c b_{n0} - \mu_n - \sum_{k=1}^{n-1} \binom{n}{k} \mu_{n-k} \lambda_k, \quad n > 1. \end{aligned} \quad (30)$$

This explicitly demonstrates how all the b_{kr} for $r \leq k \leq n$ can be expressed in terms of the b_{k0} with $k \leq n$, for arbitrary n , thus generalising the MPS result for $n = 1, 2$. This algebraic structure is clearly independent of the choice of $F(x)$ and J and also holds for peaks theory and ESP. Furthermore, the expressions above are extremely simple ways of calculating bias parameters at

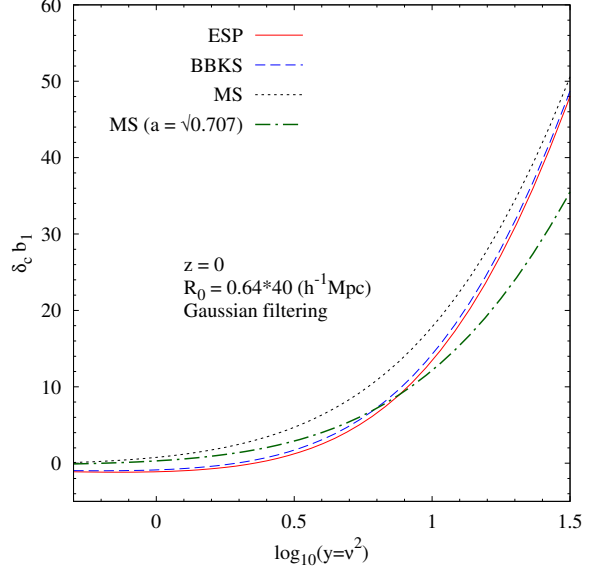


Figure 4. Linear bias predicted by peaks, excursion sets and ESP for a Gaussian filtered Λ CDM spectrum, coded as in Figure 2. The cross-correlation in equation (23) was defined on a Lagrangian scale $R_0 = 0.64 \times 40 h^{-1} \text{Mpc}$ (at which the Gaussian filter encloses the same mass as the TopHat filter at $40 h^{-1} \text{Mpc}$). Notice that whereas the replacement $\nu \rightarrow \sqrt{0.707}\nu$ in the MS mass function improved its agreement with the peaks and ESP mass functions at large masses, the same replacement under-predicts the linear bias at large masses. Interestingly, this is qualitatively similar to what is seen in N -body simulations when comparing TopHat filtered mass functions and their associated linear bias relations. See text for a discussion.

any order (compared, e.g., to the painstaking calculation in Desjacques et al. 2010 for $n \leq 2$).

Figure 4 shows the predicted linear bias for peaks, excursion sets and ESP for Gaussian filtering of the same Λ CDM spectrum and with the same colour-coding as in Figure 2, with the cross-correlation in equation (23) defined on a Lagrangian scale $R_0 = 0.64 \times 40 h^{-1} \text{Mpc}$ (at which the Gaussian filter encloses the same mass as the TopHat filter at $40 h^{-1} \text{Mpc}$). All three formalisms predict that $\delta_c b_1$ approaches $\sim (S_\times/S_0)\nu^2$ at large masses. For this reason, the modified excursion set result with $\nu \rightarrow a\nu$ (dot-dashed green) predicts a linear bias that is below the one for peaks and ESP at large masses. This is interesting because it is qualitatively the same as what has been recently found in N -body simulations: at large masses, an analytical mass function such as the one of Sheth & Tormen (1999) with $a < 1$ chosen to match the mass function of an N -body simulation *under-predicts* the linear halo bias measured in the same simulation (Manera et al., 2010; Tinker et al., 2010). This suggests that an analysis based on peaks theory such as the one presented here is on the right track towards obtaining an accurate description of both the mass function and the halo bias from first principles.

4 DISCUSSION

We showed that, especially if one accounts for correlations between steps, the standard, spherical-collapse based excursion set prediction for halo mass fractions (equation 8) vastly underestimates what is measured in simulations. However, rescaling the spherical collapse motivated self-similar scaling variable $\nu \rightarrow \sqrt{0.7}\nu$ results in much better agreement (Figure 1). We noted that this agreement should not be used to argue that halos formed from a spherical collapse – at least, not until the reason for the adhoc rescaling of ν is understood.

We then argued that the rescaling was related to a flaw in the usual formulation of the excursion set approach (Bond et al., 1991), in which one replaces an average over spatial positions in one realization of the field with an ergodic average over many independent realizations of the field. Although we are not the first to have noted this problem, much previous work has attempted to rectify this by accounting for spatial correlations between walks. However, measurements in simulations showing that halos form around special positions in the initial fluctuation field (Sheth et al., 2001) suggest that it may be more productive to instead modify the ensemble over which one computes statistical averages.

We then used peaks theory to illustrate this point, by showing how to incorporate the peaks constraint into the excursion set formalism. Specifically, peaks correspond to regions around which the curvature of the local density is modified (BBKS), and this, we argued, modifies the excursion set prediction from equation (8) to equation (16). In fact, the fundamental role played by the curvature distribution $F(x)$ (equation 13) in our analysis suggests that to build an accurate model of halo abundances, all one needs is a good model for the initial profile shapes from which halos form. For example, one might combine measurements of the density run around virialized halos with infall models to infer what the initial overdensity profiles must have been; having found them, one could use them instead of $F(x)$ in equation (16) and so predict the halo mass fraction $f(\nu)$. This is in progress.

Although our analysis has gone some way towards addressing the real cloud in cloud problem (correlated steps and correlated walks), there is more that can be done in this direction. This is because our analysis is fundamentally about taking ‘one small step’ beyond that on which the object was defined; therefore, it does not correctly account for small objects which are embedded in much more massive objects (i.e., when the smoothing scales are rather different). Some of the nicest work in this direction is in a series of papers by (Manrique et al., 1998, and references therein); we are in the process of incorporating their work into our analysis.

Our formulation of peaks in the excursion set language made it particularly easy to see how to build an excursion set model for peaks even when the question of which peaks are interesting depends on smoothing scale – the analogue of moving barriers in the excursion set approach (equation 19 and Figure 3). This may prove

necessary if one wishes to incorporate the effects of the stochasticity associated with non-spherical collapse into the excursion set peaks predictions.

The similarity in formulation also allowed a simple description of how peak abundances are modified if the large scale density field is constrained to be different in some way (equation 21). In turn, this allowed a simple generalization of earlier results on peak and halo bias to all orders (equations 26–30). In particular, we showed that excursion set peak bias is most easily understood in Fourier space, where it is k -dependent even at the linear level.

Although we concentrated on an excursion set analysis of peaks, the MS ‘one-step’ argument should apply to other traditionally single-scale analyses of cosmological datasets. For example, since the argument is not restricted to three dimensional fields, it can be applied to interpret the CMB temperature distribution, which is a two dimensional (nearly if not exactly Gaussian) random field. The number density and clustering of ‘hotspots’, as a function of spot temperature, has been used as a diagnostic of the Gaussianity of this field (Bond & Efstathiou, 1987; Heavens & Sheth, 1999). But since some hot spots will be local maxima on larger smoothing scales as well, it is of interest to describe how the distribution of sizes (and the clustering) of regions which lie above some threshold temperature depends on the value of threshold. Clearly, the analysis presented here can be applied to that problem directly. In three dimensions, perhaps the most interesting connection and application is to the series of recent papers on the ‘skeleton’ of the cosmic web (Pogosyan et al., 2009). This is the subject of ongoing work, where we hope to make a connection to the multi-scale analyses of Aragón-Calvo, van de Weygaert & Jones (2010).

Although essentially all the analysis in this paper used Gaussian smoothing filters (section 2.1 discussed why, in the present context, they simplify the analysis substantially), we do not think they are otherwise special, so we are in the process of extending our results to include tophat smoothing filters. Since fitting functions for halo counts in simulations use tophat filtering (for the conversion between σ and halo mass) exclusively, until our analysis does the same, a direct comparison with measurements of halo mass functions in simulations is premature.

This is particularly interesting in view of the fact that the linear bias factor in our excursion set peaks model is close to the usual excursion set predictions associated with rescaled δ_c at small masses, but with no rescaling of δ_c at high masses (Figure 4). This last is in qualitative agreement with measurements of halo bias in simulations. We believe that matching the enhanced abundance and bias at large masses (Figures 2 and 4), without having to rescale the parameter which is associated with the physics of halo formation, are nontrivial and encouraging successes.

ACKNOWLEDGEMENTS

We thank V. Desjacques for useful discussions. This work is supported in part by NSF-0908241 and NASA NNX11A125G. RKS thanks the GEPI and LUTH groups at Meudon Observatory for hospitality during the summer of 2012.

References

- Aragón-Calvo M. A., van de Weygaert R., Jones B. J. T., 2010, MNRAS, 408, 2163
 Appel L., Jones B. J. T., 1990, MNRAS, 245, 522
 Bagla J. S., Khandai N., Kulkarni G., 2009, MNRAS, submitted (arXiv:0908:2702)
 Bardeen J. M., Bond J. R., Kaiser N., Szalay A. S., 1986, ApJ, 304, 15
 Bond J. R., Efstathiou G., 1987, MNRAS, 226, 655
 Bond J. R., Cole S., Efstathiou G., Kaiser N., 1991, ApJ, 379, 440
 Desjacques V., Crocce M., Scoccimarro R., Sheth R. K., 2010, PRD, 82, 103529
 Heavens A., Sheth R. K., 1999, MNRAS, 310, 1062
 Ludlow A. D., Porciani C., 2011, MNRAS, 413, 1961
 Manera M., Scoccimarro R., Sheth R. K., 2010, MNRAS, 402, 589
 Matsubara T., 2011, PRD, 83, 083518
 Manrique A., Raig A., Solanes J. A., González-Casado G., Stein P., Salvador-Solé, 1998, ApJ, 499, 548
 Musso M., Paranjape A., Sheth R. K., 2012, MNRAS, accepted, arXiv:1205.3401
 Musso M., Sheth R. K., 2012, MNRAS, 423, 102
 Paranjape A., Lam T.-Y., Sheth R. K., 2012, MNRAS, 420, 1429
 Pogosyan D., Pichon C., Gay C., Prunet S., Cardoso J. F., Sousbie T., Colombi S., 2009, MNRAS, 396, 635
 Press W. H., Schechter P., 1974, ApJ, 187, 425
 Szalay A., 1988, ApJ, 333, 21
 Sheth R. K., Tormen G., 1999, MNRAS, 308, 119
 Sheth R. K., Mo H. J., Tormen G., 2001, MNRAS, 323, 1
 Sheth R. K., 2011, Pramana, 77, 169
 Tinker J. L., Robertson B. E., Kravtsov A. V., Klypin A., Warren M. S., Yepes G., Gottlöber S., 2010, 724, 878

APPENDIX A: TECHNICAL DETAILS

In this Appendix we collect technical details of various results quoted in the text.

A1 From BBKS to MPS

For Gaussian filters, the dictionary for converting between $(\tilde{\gamma}, \tilde{\nu}, \nu_p)$ and the quantities $(S_\times, \epsilon_\times, \delta_{c\times}, Q, \tilde{\delta}', \bar{\sigma})$

defined by MPS (they denoted $v \equiv d\delta/ds$ as δ') is

$$\nu_p = \frac{\delta_{c\times}}{\sqrt{sQ}}, \quad (\text{A1})$$

$$1 - \tilde{\gamma}^2 = 4s\gamma^2\bar{\sigma}^2 = \frac{\bar{\sigma}^2}{\langle v^2 \rangle} = \frac{\text{Var}(v|\nu, \delta_0)}{\text{Var}(v)}, \quad (\text{A2})$$

$$\tilde{\gamma}\tilde{\nu} = 2\gamma\sqrt{s}\tilde{\delta}' = \frac{\langle v|\nu, \delta_0 \rangle}{\sqrt{\text{Var}(v)}}, \quad (\text{A3})$$

where

$$\begin{aligned} \delta_{c\times} &\equiv \delta_c - \delta_0 \frac{S_\times}{S_0} ; \quad Q \equiv 1 - \left(\frac{S_\times}{S_0} \right)^2 \frac{S_0}{s}, \\ \tilde{\delta}' &\equiv \langle v|\nu, \delta_0 \rangle = \frac{1}{2sQ} \left[\delta_{c\times} + \epsilon_\times \frac{S_\times}{S_0} \left(\delta_0 - \delta_c \frac{S_\times}{S_0} \frac{S_0}{s} \right) \right], \\ \bar{\sigma}^2 &\equiv \text{Var}(v|\nu, \delta_0) = \frac{1}{4\Gamma^2 s} \left[1 - \frac{\Gamma^2 S_0}{Qs} \frac{S_\times^2 (1 - \epsilon_\times)^2}{S_0^2} \right], \end{aligned} \quad (\text{A4})$$

with

$$S_\times = \langle \delta\delta_0 \rangle ; \quad \epsilon_\times = \frac{2s}{S_\times} \langle v\delta_0 \rangle = 2 \frac{d \ln S_\times}{d \ln s}. \quad (\text{A5})$$

Related to these is the matrix $\tilde{\mathbf{c}}$ discussed in section 3.1, which is the quantity one must subtract from the unconditional covariance matrix of the variables (δ, v) to obtain the covariance matrix of the conditional Gaussian $p(\delta, v|\delta_0)$. This follows from equation (14) of MPS:

$$\tilde{\mathbf{c}} = \frac{S_\times^2}{sS_0} \begin{bmatrix} s & \epsilon_\times/2 \\ \epsilon_\times/2 & \epsilon_\times^2/4s \end{bmatrix}. \quad (\text{A6})$$

A2 Generalising the MPS results for bias

For the reasons mentioned in section 3.1, it is straightforward to generalise the results of MPS for halo bias to include peaks theory and its extension discussed in this work. To do this, we note that the results in their Appendices A.2 and A.3 only depend on the form of the conditional Gaussian distribution $p(\nu, x|\delta_0)$ (they work with $p(\delta, v|\delta_0)$) and not on the fact that their integrand of x used $F(x) = 1$. All that is needed then is to extend the results of their Appendix A.4 to include an arbitrary function $F(x)$ and value J in calculating the quantity $\langle \rho_h|\delta_0, \tilde{\mathbf{c}} = 0 \rangle$. With $\Gamma^2 \equiv \gamma^2/(1 - \gamma^2)$, equation (A8) of MPS can be generalised to obtain

$$\begin{aligned} \langle \rho_h|\delta_0, \tilde{\mathbf{c}} = 0 \rangle &= e^{\frac{1}{2}\nu^2 - \frac{1}{2}\nu^2(1 - \bar{\delta}_0 S_\times/S_0)^2} \\ &\times \frac{\int_0^\infty dy y^J F(y\gamma/\Gamma) p_G(y - \Gamma\nu + \bar{\delta}_0\nu_1; 1)}{\int_0^\infty dy y^J F(y\gamma/\Gamma) p_G(y - \Gamma\nu; 1)}, \end{aligned} \quad (\text{A7})$$

where we used $y = x\Gamma/\gamma$ and followed MPS in defining $\bar{\delta}_0 \equiv \delta_0/\delta_c$ and $\nu_1 \equiv \Gamma\nu(S_\times/S_0)(1 - \epsilon_\times)$.

This can also be seen more directly as follows. As MPS discussed, the condition $\tilde{\mathbf{c}} = 0$ corresponds to the assignments

$$Q \rightarrow 1 ; \quad \bar{\sigma} \rightarrow (2\Gamma\sqrt{s})^{-1} ; \quad \tilde{\delta}'/\bar{\sigma} \rightarrow (\Gamma\nu - \bar{\delta}_0\nu_1), \quad (\text{A8})$$

or

$$\begin{aligned}\nu_p &\rightarrow \nu(1 - \bar{\delta}_0(S_\times/S_0)), \\ 1 - \tilde{\gamma}^2 &\rightarrow 1 - \gamma^2, \\ \tilde{\gamma}\tilde{\nu} &\rightarrow \gamma\nu(1 - \bar{\delta}_0(S_\times/S_0)(1 - \epsilon_\times)).\end{aligned}\quad (\text{A9})$$

Making these replacements in equation (25) gives equation (A7). Taylor expanding this expression gives the bias coefficients as $\langle \rho_h | \delta_0, \tilde{\mathbf{c}} = 0 \rangle = \sum_{n=0}^{\infty} \bar{\delta}_0^n (\delta_c^n b_n) / n!$. The expansions of both Gaussians in equation (A7) involve Hermite polynomials, and lead to equation (26).